Supplemental data

In Vitro Measurement of PDE10 inhibitory activity

The test compounds were dissolved in dimethyl sulfoxide. 2 μL of the compound solution was added to a 96 well plate, and the reaction mixture (20 μL of PDE enzyme solution in 50 mM Tris-HCl, pH 8), 40 μL of the assay buffer (50 mM Tris-HCl, pH 8, 2 mM MgCl2 [12.5 mM MgCl2 used for IMA106], 0.07% 2-mercaptoethanol, and 0.825 mg/mL bovine serum albumin), and 20 μL of 1 mg/mL snake venom in 50 mM Tris-HCl (pH 8) were added to the 96 well plate. The enzyme reaction was started by adding and mixing with substrate solution of 20 μL containing approximately 7-8 nM [^{3}H]cAMP in 50 mM Tris-HCl, pH 8.0. The final concentration of cAMP in the reaction mixture was 7 nM. The reaction mixture was incubated at room temperature for 90 min. After incubation, the reaction was stopped by adding 100 μL of methanol and the resulting solution was applied to a filter plate containing Dowex (1×8 200-400) and centrifuged. 50 μL of the eluate together with an additional 100 μL methanol wash eluate were collected in another plate and the radioactivity was measured.

Radiochemistry

^{11}C-IMA107 was prepared by *N*-alkylation of the precursor IMA102.HCl using ^{11}C-methyl iodide. Enantiomeric purity of the precursor IMA102.HCl was confirmed by chiral HPLC using a CHIRALPAK® IC, 4.6 x 250 mm with a mobile phase consisting of 80% hexane, 20% ethanol and 0.1% diethylamine at a flow rate of 0.5 mL/min. Column temperature was maintained at 40°C during the analysis. IMA102 ((*R*)-5-(3-fluoropyrrolidin-1-yl)-2-(3-methylquinoxalin-2-yl)-*N*-(tetrahydro-2*H*-pyran-4-yl)pyrazolo[1,5-a]pyrimidin-7-amine) enantiomeric excess was greater than 99% as determined using reference standard of each isomer provided by Mitsubishi

Tanabe Pharma Corporation. The mild labelling conditions required for ^{11}C-IMA107 are not expected to lead to racemisation of the product.

^{11}C-Carbon dioxide was produced by the ^{14}N(p,α)^{11}C nuclear reaction using a nitrogen gas target (containing 1% oxygen) pressurised to 300-350 psi and bombarded with 11 MeV protons using the Siemens Eclipse cyclotron. Subsequently, ^{11}C-CO_2 was converted into ^{11}C-MeI by catalytic reduction (H_2/Ni) which gave the ^{11}C-CH_4 intermediate followed by gas phase iodination with iodine.

The precursor IMA102.HCl (0.5-1 mg) dissolved in dimethylformamide (400 μL) was placed in a 3 mL glass vial. 1.7 equivalents of tetrabutylammonium hydroxide (0.1M in methanol/dimethylformamide) were added. The ^{11}C-CH_3I was passed through the solution containing the precursor at room temperature using a helium stream. After delivery of ^{11}C-CH_3I, the sealed vessel was heated to 80°C for 5 min. The reaction mixture was then diluted with approximately 0.5 mL of mobile phase and injected onto the semi-prep HPLC column (Agilent XDB-C18 250 x 9.4 mm - 254 nm). HPLC purification was performed at a 8 mL/min flow rate with a mobile phase consisting of 55% acetonitrile (95% in water) and 45% ammonium formate (50 mM) adjusted to pH 8. The product fraction eluting at approximately 7.5 min corresponding to 11C-IMA107 was collected in a vial containing 25 mL of water. The resulting solution was loaded onto a Sep-Pak classic C-18 (Waters) and washed with 10 mL of water. ^{11}C-IMA107 was eluted from the cartridge using 1 mL of EtOH followed by 9 mL of 0.9% Saline solution and collected into a sterile vial. Quality control was performed on a SB-C18 150 x 4.6 mm – UV detection at wavelength λ = 254 nm using acetonitrile and a solution of ammonium formate (50mM pH 8) (55:45) as mobile phase at a flow rate of 1.5 mL/min. Identity of the radiolabelled product was confirmed by co-injection with the unlabeled IMA107 reference standard.

Radiosynthesis of ^{18}F-IMA102: ^{18}F-fluoride was produced on a Siemens RDS-111 Eclipse cyclotron by the $^{18}O(p,n)^{18}F$ reaction using a fluoride target filled with oxygen-18 enriched water. The ^{18}F-fluoride was trapped on a anion exchanger cartridge (Science Equipment Ltd®, model DW-TRC), and released with 500 µL of 10% water in acetonitrile solution, which contained 15 mg of $K_{2,2,2}$ and 3 mg of K_2CO_3. The solution containing ^{18}F-fluoride was then dried at 105°C under a nitrogen stream, 1 mL of dry acetonitrile was also added during the process. After completion, the solution of the precursor was added (around 2 mg of IMA101 in 500 µL of dry DMSO). The reaction mixture was heated for 6 min at 120°C in a vented vessel, then 1 ml of buffer (ammonium formate 50 mM pH 8) was added to quench the reaction and the mixture was injected onto a semi-preparative column for purification. ^{18}F-IMA102 was separated on an Agilent C18 column (9.4 mm x 250 mm, 5 µm) using ammonium formate 50 mM pH 8/acetonitrile (63:37) as mobile phase, at a flow rate of 8 mL/min (wavelength λ = 254 nm).

The radiochemical and chemical purity of ^{18}F-IMA102 was determined on an analytical C18 column (Agilent XDB-C18 150 mm x 4.6 mm, 5 µm) using ammonium formate 50 mM pH 8/acetonitrile (45:55) as mobile phase at a flow rate of 1.5 mL/min.

Pig PET studies

Subjects. All animal studies were performed in accordance with the Danish Animal Experimentation Act on a license granted by the Danish Ministry of Justice. Animals (pig, Yorkshire/Danish Landrace, ~40 Kg) were scanned under terminal anaesthesia (Midazolam + ketamine induced isoflurane anaesthesia). The left femoral artery and vein of each animal were surgically cannulated (Avanti size 4F-7F). Blood samples were collected from the femoral artery and the radiolabelled and non-labelled agents were injected into the femoral vein. During the

study, blood pH, pCO2 and pO2 levels were monitored and maintained within the normal physiological range. In addition, blood pressure and heart rate were recorded throughout the study.

PET Data Acquisition. PET imaging was performed on a Siemens ECAT EXACT HR tomograph, with the head immobilised in a custom-made holding device. Prior to each emission scan a transmission scan of 10 minutes was performed using 3 rotating 68Ge-68Ga sources. The information was used for attenuation correction. Each animal received an intravenous bolus injection of the tracer. Dynamic emission data were collected in the 3D mode for 90 min as 26 successive frames of increasing duration (8 x 0.25 min, 4 x 0.5 min, 2 x 1 min, 2 x 2 min, 4 x 5 min, 6 x 10 min). Data were reconstructed using a reprojection algorithm with an axial and transaxial Hanning filter with a 0.5 cut-off frequency.

Image Processing. For each study, the baseline PET summed image was co-registered using a 12-parameter affine registration to a Landrace pig brain atlas using a mutual information cost function. T1-weighted MR scans from 22 female Yorkshire Landrace pigs were used to generate the atlas using methods described previously for the Gottingen minipig (1). Subsequently, the transformation parameters were applied to the dynamic PET sequence and regional time activity curves (TACs) were derived by application of the anatomically parcellated template. The following regions of interest (ROIs) were defined: striatum, frontal cortex, cerebellum and diencephalon. All registrations were assessed by visual inspection.

The blocking experiments were conducted using IMA102 administered as an intravenous bolus injection over 1 minute, 5 minutes prior to tracer injection. IMA102 was dissolved in 0.9% w/v saline.

Baboon PET study

Subjects. The study was approved by the local Institutional Animal Care and Use Committee (IACUC). PET imaging was carried out on four adult female baboons (Papio Anubis) weighing on average 13.2 ± 1.1 kg. Fasted animals were immobilized with ketamine (10 mg/kg i.m.), and anesthetized with 1.5-2.5% isoflurane via an endotracheal tube. Vital signs were monitored every 15 min and the temperature was kept constant at ~37 °C with heated water blankets. An intravenous perfusion line was used for hydration and injection of the radiotracer. A catheter was inserted in a femoral artery for arterial blood sampling.

PET Data Acquisition. PET imaging was performed with the ECAT EXACT HR+ PET scanner (Siemens/CTI, Knoxville, TN). The head was positioned at the centre of the field of view using a laser positioning system. A 6-min transmission scan was obtained prior to radiotracer injection for attenuation correction. The radiotracer was injected intravenously over 3 min in ethanol/saline into the femoral vein. Average activity injected was 152 MBq ± 24 MBq (n = 16), 127 MBq (n = 1), and 173 MBq ± 3 MBq (n = 4) for ^{11}C-MP-10, ^{11}C-IMA106, and ^{11}C-IMA107, respectively. Average mass of unlabelled tracer injected was 0.08 ± 0.07 μg/kg (n =16), 0.24 μg/kg (n = 1), and 0.11 ± 0.04 μg/kg (n = 4) for ^{11}C-MP-10, ^{11}C-IMA106, and ^{11}C-IMA107, respectively. Dynamic emission data were acquired over a period of 120 min. Dynamic images (33 frames) were reconstructed from sinograms with an attenuation-weighted OSEM algorithm.

Image Processing. Inter-modality registrations (PET-to-MRI) were performed using an automated process based on normalized mutual information (NMI) (*2*). Individual MRIs were

also warped to a baboon MRI template using a linear and nonlinear registration. The template MRI was created by averaging individual baboon MR images that were spatially normalized using a NMI linear and nonlinear registration. The following ROIs were delineated on the baboon template image: putamen, caudate, globus pallidus, nucleus accumbens, frontal cortex, occipital cortex, cingulate, insula, cerebellum, thalamus, pons, and brainstem. Transformation parameters from the individual registrations (template-to-MRI and MRI-to-PET) were combined and applied to the PET dynamic data to derive time-activity curves for each ROI.

Arterial Plasma Input Function Generation. The input functions corresponding to the arterial blood plasma concentration corrected for the presence of radio-metabolites were generated for all scans and all tracers. Arterial blood samples (0.5-4 mL) were collected at 3, 8, 15, 30, 60 and 90 min after tracer injection. The blood was centrifuged and the plasma separated. Plasma metabolite analysis was performed using the column switching method (*3*). Plasma samples treated with urea (8 M) to eliminate plasma protein binding were loaded onto the capture column (19 x 4.6 mm) self-packed with Phenomenex SPE C18 Strata-X sorbent with 1% acetonitrile in water at 2 mL/min. The trapped activity was eluted through the analytical column (Phenomenex Luna C18(2) analytical column [250 x 4.6mm, 5µm]) using a mobile phase consisting in acetonitrile and 0.1M ammonium formate pH 6.4 at 1.5 mL/min, with 55% of acetonitrile for ^{11}C-MP-10 and ^{11}C-IMA107 and 65% of acetonitrile for ^{11}C-IMA106. The fraction of unchanged tracer was determined by integration of the peak corresponding to the parent compound and expressed as percentage of all the radioactive peaks observed.

Blocking Experiments. Blocking experiments were conducted using 0.6 and 1.8 mg/kg doses of MP-10 formulated as previously described (9) and administered i.v. as a 30 min infusion. The post-dose tracer scan was started 5 min after the end of the infusion.

Tracer Kinetic Analysis. Quantitative compartmental analysis was explored using one and two tissue compartment models with a plasma input function. Across the 3 tracers and in control and blocking studies, the two tissue compartmental model was more appropriate than the one tissue compartmental model, based on the F test ($p < 0.05$). Also, the uncertainty (% standard error) of the volume of distribution (V_T) estimates was generally small (typically < 5%), therefore for brevity, only these results are presented. The influx rate constant, K_1, was also estimated and averaged across all regions for all the baseline scans and for the post-pharmacological challenge scans. The cerebellar V_T, which showed no signs of blocking following administration of a selective PDE10A inhibitor, was used as a measure of non-displaceable volume of distribution (V_{ND}). This enabled calculation of the binding potential ($BP_{ND} = \frac{V_T - V_{ND}}{V_{ND}}$, which is proportional to the ratio B_{max}/K_d) for each region of interest. The regional target occupancy (*Occ*) following blockade with the unlabelled MP-10 was calculated as the relative change in BP_{ND} and refers to the percentage of the enzyme bound by the drug molecule:

$$Occ = \frac{BP_{ND}^{baseline} - BP_{ND}^{drug}}{BP_{ND}^{baseline}}$$

The occupancy values were averaged across the striatal regions (putamen and caudate) to estimate the percent occupancy.

REFERENCES

1. Watanabe H, Andersen F, Simonsen CZ, Evans SM, Gjedde A, Cumming P. MR-based statistical atlas of the Gottingen minipig brain. Neuroimage 2001;14:1089-1096.

2. Sandiego CM, Weinzimmer D, Carson RE. Optimization of PET-MR registrations for nonhuman primates using mutual information measures: a multi-transform method, *Neuroimage* 2013;64:571-581.

3. Hilton J, Yokoi F, Dannals RF, Ravert HT, Szabo Z, Wong DF. Column-switching HPLC for the analysis of plasma in PET imaging studies. Nucl Med Biol. 2000;27:627-630.

SUPPLEMENTAL TABLE 1. Affinity of IMA107 for various receptors, enzymes, ion channels and transporters.

Receptors, channel or transporter	Radioligand	Source	IMA107	
			% Inh.* (10 μM)	IC_{50} (μM)
Adenosine A1	[^{3}H]DPCPX	Human recombinant CHO cells	36	
Adenosine A_{2A}	[^{3}H]CGS-21680	Human recombinant HEK-293 cells	9	
Adrenergic α_{1A}	[^{3}H]Prazosin	Wistar Rat submaxillary gland	21	
Adrenergic α_{1B}	[^{3}H]Prazosin	Wistar Rat liver	10	
Adrenergic α_{2A}	[^{3}H]MK-912	Human recombinant insect Sf9 cells	0	
Adrenergic β_1	[^{125}I]Cyanopindolol	Human recombinant CHO-K1 cells	2	
Adrenergic β_2	[^{3}H]CGP-12177	Human recombinant CHO cells	6	
Ca Channel L-Type, dihydropyridine	[^{3}H]Nitrendine	Wistar Rat cerebral cortex	6	
Dopamine D_1	[^{3}H]SCH-23390	Human recombinant CHO cells	11	
Dopamine D_{2s}	[^{3}H]Spiperone	Human recombinant CHO cells	14	
GABA $_A$, Flunitrazepam, Central	[^{3}H]Flunitrazepam	Wistar Rat brain (minus cerebellum)	5	
GABA $_A$, Muscimol Central	[^{3}H]Muscimol	Wistar Rat brain (minus cerebellum)	-4	
Glutamate, NMDA, phencyclidine	[^{3}H]TCP	Wistar Rat cerebral cortex	2	
Histamine H_1	[^{3}H]Pyrilamine	Human recombinant CHO-K1 cells	8	
Imidazoline I_2, Central	[^{3}H]Idazoxan	Wistar Rat cerebral cortex	-6	
Muscarinic M_2	[^{3}H]N-Methylscopolamine	Human recombinant CHO-K1 cells	-8	
Muscarinic M_3	[^{3}H]N-Methylscopolamine	Human recombinant CHO-K1 cells	7	
Nicotinic Acetylcholine	[^{125}I]Epibatidine	Human IMR-32 cells	-35	
Nicotinic Acetylcholine α_1, Bungarotoxin	[^{125}I]α-Bungarotoxin	Human RD cells	4	
Opiate (μOP3, MOP)	[^{3}H]Diprenorphine	Human recombinant CHO-K1 cells	7	
Phorbol Ester	[^{3}H]PDBu	ICR Mouse brain	-6	
Potassiun Channel [K_{ATP}]	[^{3}H]Glyburide	Hamster pancreatic HIT-T15beta cells	-2	
Potassiun Channel hERG	[^{3}H]Astemizole	Human recombinant HEK-293 cells	20	
Prostanoid EP_4	[^{3}H]Prostaglandin	Human recombinant Chem-1 cells	11	
Rolipram	[^{3}H]Rolipram	Wistar Rat brain	28	
Serotonin 5-HT_{2B}	[^{3}H]Lysergic acid	Human recombinant CHO-K1 cells	57	5.84
Sigma δ_1	[^{3}H]Haloperidol	Hunan jurkat cells	21	
Sodium Channel, Site 2	[^{3}H]Batrachotoxin	Wistar Rat brain	38	
Transporter, norepinephrine (NET)	[^{125}I]RTI-55	Hunan recombinant MDCK cells	9	
Bradykinin B_2	[^{3}H]Bradykinin	Hunan recombinant Chern- I cells	9	
Cannabinoid CB_1	[^{3}H]SR141716A	Human recombinant Chern-I cells	3	
Cannabinoid CB_2	[^{3}H]WIN55,212-2	Human recombinant CHO-K1 cells	5	
GABA $_A$ (Chloride channel, TBOB)	[^{3}H]TBOB	Wistar Rat cerebral cortex	7	
Glutamate (Non-selective)	[^{3}H]L-Glutamic acid	Wistar Rat brain	9	
Glycine (Strychnine-Sensitive)	[^{3}H]Strychnine	Wistar Rat spinal cord	0	
Histamine H_2	[^{125}I]Aminopotentidine	Human recombinant CHO-K1 cells	9	
Muscarinic M_1	[^{3}H]N-Methylscopolamine	Human recombinant CHO-K1 cells	8	
Opiate (Non-selective)	[^{3}H]Naloxone	Wistar Rat brain	7	
Serotonin $5HT_{1A}$	[^{3}H]8-OH-DPAT	Human recombinant CHO-K1 cells	12	
Serotonin $5HT_{2A}$	[^{3}H]Ketanserin	Human recombinant CHO-K1 cells	0	
Serotonin $5HT_3$	[^{3}H]GR-65630	Human recombinant HEK-293 cells	4	
Transporter, Dopamine transporter (DAT)	[^{125}I]RTI-55	Human recombinant CHO-K1 cells	6	
Transporter, Serotonin transporter (SERT)	[^{3}H]Paroxetine	Human recombinant HEK-293 cells	8	

* % inh. represents the percentage of inhibition at a 10 μM concentration

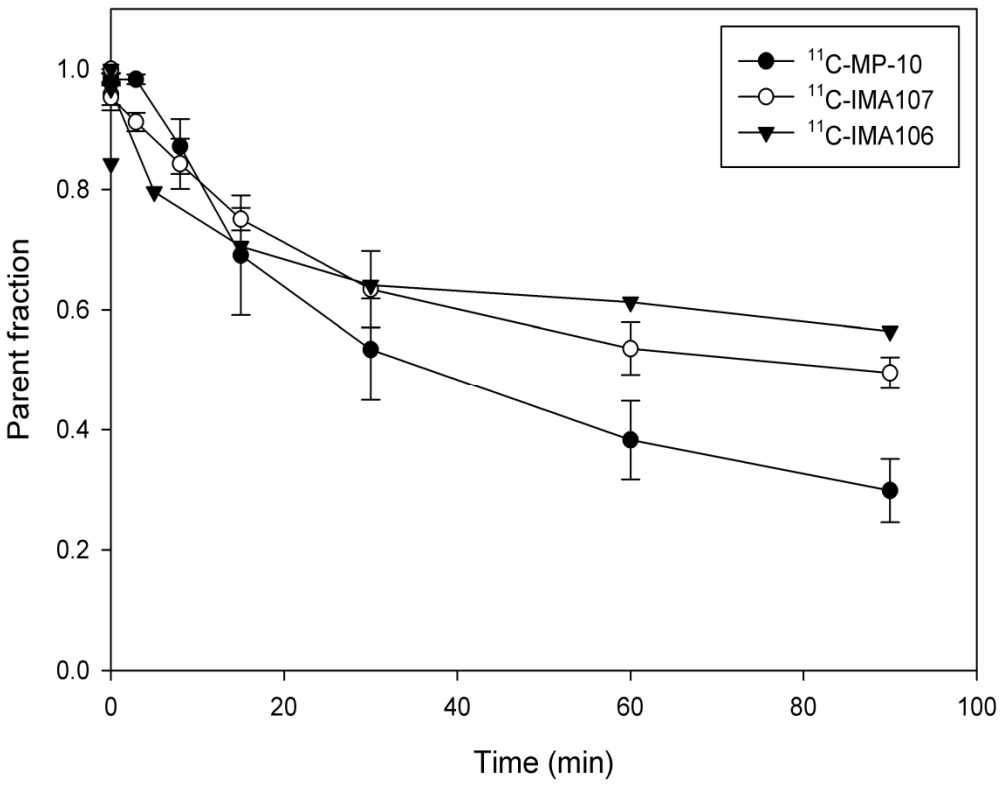

Supplemental FIGURE 1. In vivo metabolism of ^{11}C-MP-10 (n = 16), ^{11}C-IMA106 (n = 1) and ^{11}C-IMA107 (n = 4) in the baboon. The error bars represent the standard errors of the mean.

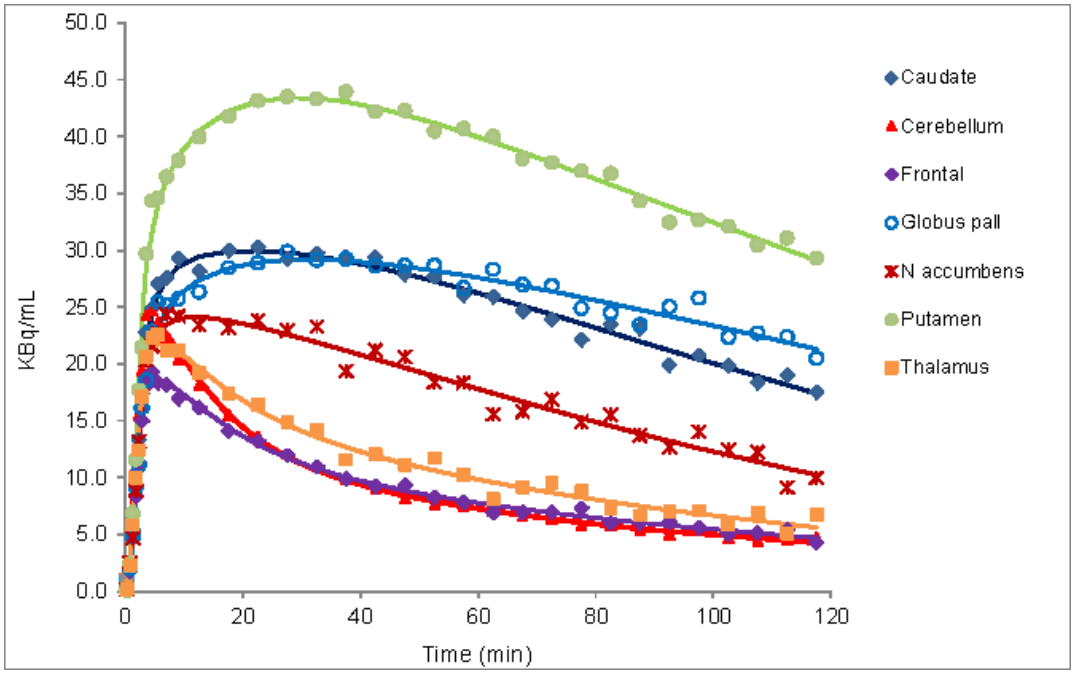

Supplemental FIGURE 2. Time-activity curves describing the kinetics of ^{11}C-IMA107 for selected ROIs in baboon brain. Points are the measured values and lines are the 2TC model fits.